phys. stat. sol. (a) **188**, No. 4, 1495–1503 (2001)

Sum Frequency Generation Study of CO Adsorption on Palladium Model Catalysts

H. UNTERHALT, P. GALLETTO[1]), M. MORKEL, G. RUPPRECHTER, and H.-J. FREUND

Fritz-Haber-Institut der Max-Planck-Gesellschaft, Chemical Physics Department, Faradayweg 4–6, D-14195 Berlin, Germany

(Received August 17, 2001; in revised form September 14, 2001; accepted September 19, 2001)

Subject classification: 68.43.Fg; 68.47.De; 68.47.Jn; 78.40.Kc; S1.3

In the present contribution CO adsorption on palladium aggregates was examined with IR-visible sum frequency generation vibrational spectroscopy. Supported Pd nanoparticles of different mean size and surface roughness were prepared by electron beam evaporation on an ordered Al_2O_3 thin film formed on NiAl(110). SFG spectra were acquired for a wide range of CO pressures (from 1×10^{-7} to 200 mbar) at 190 to 300 K. At low pressure, evidence for a particle structure dependence of the CO adsorption geometry was found, with on-top CO sites significantly occupied on defective particles. On the other hand, under a high pressure regime, discrepancies between rough and smooth well-faceted particles were mostly reduced, with the relative fraction of on-top CO nearly equal for both cases. As a reference model, adsorption on well-defined Pd(111) single crystals was monitored as a function of CO pressure up to 1 bar and contrasted to the work done on aggregates. Under ultrahigh vacuum the SFG spectra on large Pd particles closely resembled the Pd(111) response. However, for pressures higher than 1 mbar at 190 K twofold bridge bonded sites were no longer populated on the Pd(111) surface while the bridge bonded occupancy was significant on Pd aggregates for all pressures studied.

1. Introduction

To a great extent, the use of second harmonic generation (SHG) and sum frequency generation (SFG) has been stimulated by the aim of gaining specific knowledge of surface properties [1, 2]. As second order non-linear optical processes, SHG and SFG are forbidden in media with inversion symmetry under the electric dipole approximation, but allowed at the surface where the inversion symmetry is broken [3]. As a consequence, both methods can be employed to probe the interfacial region between two isotropic media, provided the interface is accessible by light. Compared to SHG, SFG constitutes a more direct probe for adsorbed species and/or the surface layer, because of its molecular specificity [1]. Like IR and Raman spectroscopies, IR-visible SFG probes adsorbate molecular vibrational modes and therefore is able to provide information on the molecular interactions and orientations at the surface. SFG has been used to probe solid–gas interaction [2, 4] but also buried interfaces such as solid/liquid and liquid/liquid interfaces were examined [5, 6].

For instance, SFG studies in electrochemistry have contributed to the understanding of the effect of the strong interfacial electric field onto the nature of the adsorbate/metal (electrode) interaction [7–9]. Interference phenomena between the resonant signal from the adsorbed molecules and the nonresonant background occur [9–11] and, as a result, the line shape of the measured SFG signal can vary depending on the relative

[1]) Corresponding author; Phone: +49 30 8413 4143; Fax: +49 30 8413 4315;
e-mail: galletto@fhi-berlin.mpg.de

© WILEY-VCH Verlag Berlin GmbH, 13086 Berlin, 2001 0031-8965/01/18812-1495 $ 17.50+.50/0

phase of both contributions. This effect is specifically relevant for metals, where the nonresonant signal strength can reach the same order of magnitude as the resonant term. Interesting surface properties, such as the point of zero charge for electrochemical interfaces, could be estimated by measuring the phase difference between the nonresonant and resonant contributions as a function of the applied potential [9]. Furthermore, the visible frequency and/or the SFG frequency may be resonant with electronic transitions of the substrate or the adsorbate. In this case, infrared/visible SFG, differently from linear techniques or SHG, allows one to probe simultaneously vibrational modes and electronic structure [9–11].

In recent years considerable effort in the field of catalysis has been directed toward the use of techniques which are suitable to work under technically relevant conditions, that means at elevated pressure and temperature [4, 12–18]. One of the questions addressed was the applicability of surface science studies under ultrahigh vacuum (UHV) to catalysis. The presence of a gas phase at higher temperature may produce adsorbate geometries different from UHV conditions. In addition, there has been evidence that the catalyst surface may be subjected to reconstruction upon exposure to high pressure [19, 20] and intermediate species be present only during catalytic reactions [4]. The interest to narrow the gap between high pressure and traditional surface science experiments has promoted SFG, among other methods, as an ideal tool to examine adsorption and follow reactions under catalytic conditions.

In the present contribution, infrared-visible SFG was utilized to investigate the chemisorption of CO on oxide supported Pd nanoparticles and on Pd(111) up to 1 bar, with the single crystal serving as reference. The experiments were carried out over a wide range of pressure utilizing particle distributions with different mean size and morphology.

2. Experimental

Vibrational spectroscopy on Pd particles was performed using the SFG setup described in detail elsewhere [21]. An amplified Ti-sapphire laser supplied 790 nm radiation (2 ps pulses at a repetition rate of 500 Hz) used as visible light for the experiment and as pump for the infrared generation. The tunable infrared light was produced by an optical parametric amplifier (OPA)/difference frequency generator (DFG) system, producing an approximately constant power between 2000 cm^{-1} and 3300 cm^{-1} ($\sim$10 μJ/pulse; 25 cm^{-1} resolution). Below 1900 cm^{-1}, the infrared power was smaller thus precluding SFG investigations in this spectral region.

A different laser source, consisting of a Nd:YAG laser with 25 ps pulse duration and a repetition rate of 50 Hz was employed to investigate Pd(111). The YAG output at 1064 nm was split into two beams. One was frequency doubled to produce green light at 532 nm. The other was used to pump an improved OPA/DFG system for the tunable infrared light. This OPA/DFG offered better spectral resolution and increased IR power below 1900 cm^{-1} ($\sim$150 μJ/pulse; 5 cm^{-1} resolution). It is worth noting that the visible frequency at 790 nm produced by the Ti-sapphire laser source was far from any resonance with electronic transitions typical of palladium and/or of NiAl. Also, the resonant SFG signal was higher than the nonresonant background, with a phase between them leading to rather symmetric SFG peaks.

In both experimental configurations, the input visible and infrared beams were vertically polarized and were allowed to impinge at the surface with an incident angle of

50 ° and 55 ° respectively. Temporal and spatial overlap was controlled by optimizing the SFG signal generated by the substrate and/or CO. The output SFG beam was left unpolarized and passed to a monochromator and detected via a photomultiplier tube and a boxcar averager. Calibration of the incident infrared light was checked by monitoring CO_2 stretching vibrations around 2350 cm^{-1}. The SFG signal generated from the sample surface was either normalized to the response of a GaAs reference crystal which produces a constant bulk SFG signal over the investigated spectral region, or to the incident IR intensity on the surface, calculated from the measurement of the reflected IR energy [22]. This allowed to minimize shot-to-shot fluctuations in the laser power. A GaAs reference was also placed at the sample position inside the high pressure cell to determine IR absorption through the CO gas phase, thus allowing correction of the raw data [16, 23].

The experiments were performed in a two level system suitable for UHV and high pressure studies [21, 23]. The UHV chamber with a base pressure of 1×10^{-10} mbar was used for sample preparation and characterization (e.g. by low energy electron diffraction or Auger spectroscopy). The preparation of supported Pd nanoparticles is explained in detail in [24]. Briefly, an ordered aluminum oxide film was grown by oxidizing a NiAl(110) substrate. Then, Pd was deposited by electron beam evaporation. The mean Pd particle size and (surface) structure were adjusted by controlling the substrate temperature during deposition and the amount of deposited metal. Particles of 3.5 nm mean size were grown on Al_2O_3 at 90 K by depositing a nominal Pd thickness of 0.6 nm, whereas 7.5 nm particles were formed by depositing 1 nm Pd at 300 K.

Following the standard procedure of cutting and polishing, Pd(111) surfaces were prepared by sequences of Ar ion bombardment (beam energy 1 kV at 3×10^{-4} mbar Ar), annealing to 1200 K and oxidation between 1200 and 600 K in 5×10^{-7} mbar O_2, followed by a final flash to 1200 K [22]. The surface cleanliness and structure were examined with Auger and LEED.

After preparation in UHV the samples were moved with a manipulator into the SFG UHV-high pressure cell [21]. The cell has CaF_2 windows and is suitable for SFG studies from UHV to 1 bar. During the transfer, the sample holder is introduced into three differentially pumped teflon seals, thus separating the UHV from the high pressure section during SFG experiments. This is essential to avoid contamination of the preparation level. CO was introduced via a cold trap filled with a liquid nitrogen/ethanol mixture (ca. 170 K) to remove Ni- and Fe-carbonyl impurities, which would otherwise become relevant at elevated CO pressure [23].

3. Results

CO on Pd(111) has been frequently studied by infrared reflection absorption spectroscopy (IRAS) [25–28] while SFG was only applied at low pressure [29]. In the following, we will first discuss results on Pd(111) since, beside providing a good reference, it allows us to compare SFG with IRAS. The second part will be dedicated to the adsorption of CO on Pd nanoparticles.

3.1 CO on Pd(111)

Surface science studies typically achieve high (saturation) coverages by successively exposing CO at low temperature. For instance, at 100 K several Langmuirs or 10^{-7} mbar CO were sufficient to produce saturation (0.75 ML) on Pd(111) [25–28]. At higher

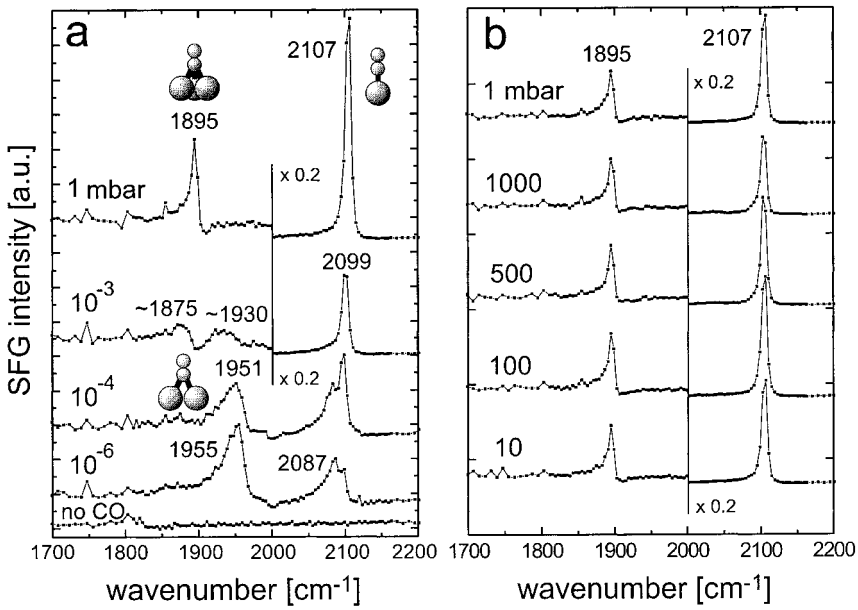

Fig. 1. a) SFG spectra of CO adsorption on Pd(111) at 190 K, from 10^{-6} to 1 mbar. Between 10^{-3} and 1 mbar a transition from a bridge/on-top to a hollow/on-top configuration takes place; b) SFG spectra of CO adsorption on Pd(111) at 190 K, from 10 to 1000 mbar. The last spectrum at 1 mbar illustrates the reversibility of the spectra

temperature, the saturation coverage may not be obtained under UHV, but only when the pressure is significantly increased ($\sim$1 mbar). This is illustrated in Fig. 1 showing SFG spectra of CO on Pd(111) at 190 K. The first measurement was conducted without CO and shows the nonresonant background. The background signal is related to the electron density profile at the Pd surface and was found to be invariant with IR frequency. Upon dosing CO, SFG spectra showed CO adsorbed in bridge-bonded and on-top sites which progressively turned into a combination of hollow and on-top CO. First CO resonances could be observed at 10^{-6} mbar CO at 1955 cm^{-1} and 2087 cm^{-1} (Fig. 1a), which were assigned to bridge bonded and on-top species. The on-top peak was found to increase with coverage, whereas the intensity of the bridge bonded signal decreased. At 10^{-6} and 10^{-4} mbar two on-top species could be distinguished. Beside the 2087 cm^{-1} resonance there was a peak at 2099 cm^{-1} which finally shifted to 2107 cm^{-1}. It is possible that the 2087 cm^{-1} peak originates from CO linearly bound to steps or defects and that the 2099 cm^{-1} peak is due to on-top CO on the (111) terraces. Transition from bridge/on-top (0.63 ML) to hollow/on-top (0.75 ML) occupancy [25] occurred above 10^{-3} mbar (Fig. 1a). The 0.75 ML coverage was fully attained with a CO pressure of 1 mbar at 190 K. Further increase in pressure leads to an enhancement of the CO on-top resonance (Fig. 1b). For pressures higher than 500 mbar, no more frequency shifts were observed and the hollow peak remained constant, but the on-top signal was reduced. The decrease of the on-top signal is probably related to some uncertainty in the IR normalization above 500 mbar and does not reflect a real disappearance of on-top CO. For a reason yet unknown the IR intensity on the surface at high pressure is

presumably smaller than that inferred from measurement of the reflected IR light. The 1 mbar spectrum was recorded once more at the end of the high pressure measurements and the previous spectrum could be perfectly reproduced (Fig. 1b). This indicates that no pronounced irreversible surface transformations or contamination were present under high pressure conditions.

Combined IRAS and LEED investigations performed on the Pd(111) system [25–28] have shown that the binding site progression with increasing coverage mainly consisted of a gradual change from threefold hollow sites to bridge bonded sites and finally to a combination of on-top and threefold hollow sites. For a coverage θ = ~0.3, the $(\sqrt{3} \times \sqrt{3}) - R\,30^\circ$ structure was formed with CO adsorbed on threefold hollow sites. The latter assignment was given on the basis of IRAS findings, namely from the appearance of a low frequency band located at 1836 cm^{-1}. The threefold hollow signal at low coverage could not be observed with SFG probably because of the low Raman polarizability of threefold coordinated CO, resulting in a rather weak signal that could not be distinguished from the smeared out response of Pd electrons. Higher coverages (~0.5 ML) were shown to give rise to a broad band around 1930 cm^{-1}, which was originally attributed to CO arranged in twofold bridge sites. However, recent photoemission and photoelectron diffraction studies [30,31] have proved the initial assignment to be incorrect, with CO instead adsorbing on threefold hollow sites. With increasing coverage up to 0.6–0.7 ML, the dominant feature is that of bridge bonded CO (~1960 cm^{-1}) with a small amount of terminal CO (~2090 cm^{-1}). If the coverage is further increased to saturation (θ = 0.75), two intense bands are observed at 1895 cm^{-1} and 2110 cm^{-1}, respectively assigned to hollow and on-top site occupancy.

While there is a good agreement in the resonance frequencies observed by SFG and IRAS, when the relative intensities of hollow, bridge and on-top signals are considered, only qualitative agreement is obtained. The weak SFG signals of hollow and bridged CO as compared with IRAS findings are probably related to the low Raman polarizability specific of multiple-coordinated CO [32–34] or may originate from an interference effect between different SFG susceptibility tensor elements as shown by Baldelli et al. [35].

3.2 CO on Pd nanoparticles

SFG spectra of adsorbed CO were acquired on Pd aggregates of different mean size. As mentioned in the experimental section, by controlling the substrate (alumina) temperature during Pd deposition, the mean particle size can be adjusted. As already told, the Pd particles grown at 300 K have an average size of 7.5 nm (about 7000 atoms per particle, 1×10^{12} particles/cm^2). They were found to be crystalline, with cuboctahedral shape and well defined facets [24, 36]. Their morphology is dominated by a (111) top facet (oriented parallel to the substrate), with smaller contribution from (111) and (100) side facets. CO adsorbed on the side facets is tilted with respect to the plane of the underlying substrate and according to the IR selection rule, the contribution from tilted CO should be relatively small.

SFG measurements on 7.5 nm particles were performed for several CO pressures ranging from 10^{-7} to 100 mbar at 190 to 300 K (Fig. 2). For a CO pressure of 10^{-7} mbar and 190 K, a pronounced band is observed at 1985 cm^{-1} and assigned to bridge bonded CO, whereas the signal originating from on-top CO was much smaller

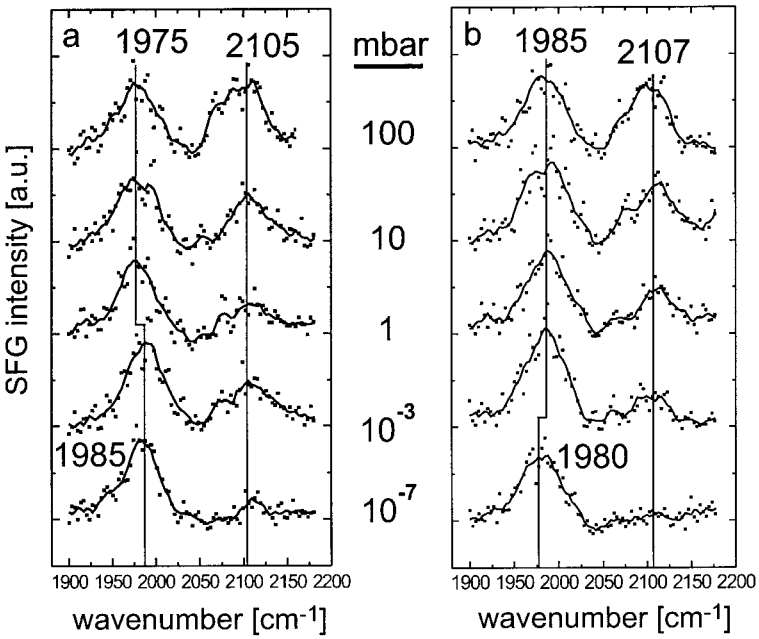

Fig. 2. CO adsorption on Pd/Al_2O_3 (mean particle size 7.5 nm) as monitored by SFG at a) 190 K and b) 250 K, in a pressure range from 10^{-7} mbar to 100 mbar CO. For both temperatures the fraction of on-top CO is very small under UHV but can be significantly increased with increasing pressure

(Fig. 2a), in agreement with previous IRAS data [37, 38]. The resonance frequency of 1985 cm^{-1} is different from the Pd(111) value of 1955 cm^{-1}. In light of recent SFG spectra obtained from "defect-rich" (strongly sputtered) Pd(111) we suggest the peak at 1985 cm^{-1} to be related to CO adsorption on surface steps and/or particle edges [22]. As shown by HRTEM and STM [19, 38] monoatomic steps are even present on well-faceted nanoparticles. IRAS had shown a third weaker band around 1950 cm^{-1} that was assigned to CO bridge bonded on (111) terraces. It was not possible to detect the weaker species with SFG since the defect-related species dominates over CO bridge bonded on terraces. It is also possible that the resulting twofold coordinated CO SFG signal originates from the coupling between CO molecules bound to steps/defects and those adsorbed on terraces [39]. Similar IR spectra were also reported for Pd/Al_2O_3/Ta(110) model catalysts [40] and for impregnated Pd/SiO_2 [41].

With increasing pressure, the on-top SFG signal strongly increased. This behavior is in agreement with the results obtained on Pd(111). However, while bridge bound CO disappeared on Pd(111) around 1 mbar, this species persisted even up to 100 mbar on the Pd aggregates. As already mentioned earlier, the hollow site region could not be properly investigated because of the drop of the IR power for frequencies below 1900 cm^{-1}.

When the same spectra were taken at 250 K (Fig. 2b) and 10^{-7} mbar, bridge bound CO was still the dominant species with on-top CO nearly reduced to the noise level. This can be understood on the basis of thermal desorption spectroscopy showing that on-top CO desorbs around 250 K [24]. However, on-top CO reappears with increasing pressure, giving rise to a very similar on-top/bridge bonded CO pattern for high pressure as found for the same particles at 190 K.

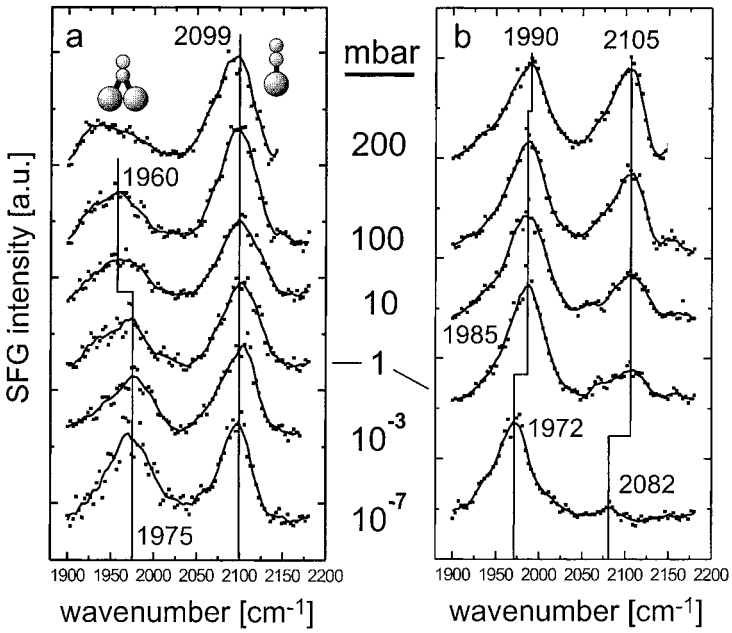

Fig. 3. CO adsorption on Pd/Al_2O_3 (mean particle size 3.5 nm) as monitored by SFG at a) 190 K and b) 300 K, in a pressure range from 10^{-7} mbar to 200 mbar CO. At 300 K the fraction of on-top CO is much reduced but these sites can be repopulated with increasing pressure

The same measurements were also carried out on Pd particles with a mean diameter of 3.5 nm (about 850 atoms per particle). It should be noted that these particles are not only smaller but also grown at a lower substrate temperature (90 K), resulting in a higher nucleation density (5×10^{12} particles/cm^2) and Pd aggregates with less-ordered surfaces. The total Pd surface area of the 3.5 nm Pd particle sample was about 20% bigger than in the 7.5 nm case and partly accounts for the better signal-to-noise ratio in Fig. 3 (beside day-to-day performance of the laser and the OPG). The pressure series at 190 K is given in Fig. 3a. At 10^{-7} mbar two peaks were again observed, corresponding to bridge bonded CO (1975 cm^{-1}) and to on-top CO (2099 cm^{-1}). It is striking that at 10^{-7} mbar, the fraction of adsorbed on-top CO is much higher than for the previous case of larger particles. This finding indicates that smaller Pd aggregates possess a highly defective structure corroborating IRAS data gathered on Pd particles and rough Pd thin films [26, 37]. The pattern with coexisting bridge bonded and on-top features was maintained even up to 200 mbar. With increasing pressure the signal of bridge bonded CO decreased in intensity and moved gradually to lower frequencies, but without vanishing at high pressure. The transition to the hollow/on-top configuration was only partial manifesting itself as a decrease of the bridge bonded CO response, whereas on Pd(111) the same transition occurred at much lower CO pressure ($\sim$1 mbar) with a well resolved hollow/on-top CO pattern (cf. Fig. 1).

When increasing the temperature to 300 K, the adsorption behavior appeared to be significantly different, with the most striking feature being a very weak on-top CO peak. This can again be understood considering the desorption of on-top CO. To obtain an adsorption site occupancy similar to the 10^{-7} mbar/190 K spectrum, a pressure of

about 200 mbar is necessary at 300 K. In contrast to Figs. 2a and 3a there was no decrease of the bridge intensity indicating that we are far from conditions where a phase transition to a hollow/on-top structure would occur.

4. Conclusion

The present SFG study performed on Pd nanoparticles allows us to emphasize the influence of particle size and structure on the nature of CO adsorption sites. By comparing $Pd/Al_2O_3/NiAl(110)$ model catalysts consisting of smaller and larger metal particles different adsorption patterns were observed under UHV conditions ($\sim 10^{-7}$ mbar). For small 3.5 nm particles that exhibited rough surfaces, bridge bonded and on-top species coexisted giving rise to comparable SFG signals. In contrast, on larger well-faceted Pd particles the SFG spectrum showed a strongly dominating bridge-bonded feature. In both cases the observed bridge species was related to adsorption on step/edge sites. However, when the pressure was increased to values typical of catalytic reactions, a combination of two-fold bridge bonded and on-top CO was observed, independent of the particle size. It appears that the structural differences steering adsorption under UHV did have a much smaller effect at 200 mbar CO.

A more complete picture of the structure dependent CO adsorption on Pd was obtained after investigation of Pd(111) under the same experimental conditions. In contrast to Pd particles, the bridge bonded feature disappeared above 1 mbar at 190 K resulting from a rearrangement of the adsorbate layer from a bridge/on-top to a hollow/on-top configuration. This transition did not (fully) occur on the Pd nanoparticles presumably because on their curved surfaces of limited size the necessary lateral CO interactions cannot be established.

References

[1] Y. R. SHEN, Nature **337**, 519 (1989).
[2] R. B. HALL, J. N. RUSSELL, J. MIRAGLIOTTA, and P. R. RABINOWITZ, Chemistry and Physics of Solid Surfaces, Springer Series in Surface Science, Vol. 22, Eds. R. VANSELOW and R. HOWE, Springer-Verlag, Berlin 1990 (p. 87).
[3] Y. R. SHEN, The Principles of Nonlinear Optics, John Wiley, Inc., 1984.
[4] G. A. SOMORJAI and G. RUPPRECHTER, J. Phys. Chem. B **103**, 1623 (1999).
[5] G. L. RICHMOND, Ann. Rev. Phys. Chem. **52**, 357 (2001).
[6] K. B. EISENTHAL, Chem. Rev. **96**, 1343 (1996).
[7] C. MATRANGA and P. GUYOT-SIONNEST, J. Chem. Phys. **112**, 7615 (2000).
[8] W. DAUM, F. DEDERICHS, and J. E. MÜLLER, Phys. Rev. Lett. **80**, 766 (1998).
[9] A. TADJEDDINE, A. LE RILLE, O. PLUCHERY, F. VIDAL, W. Q. ZHENG, and A. PEREMANS, phys. stat. sol. (a) **175**, 89 (1999).
[10] X. D. ZHU, H. SUHR, and Y. R. SHEN, Phys. Rev. B **35**, 3047 (1987).
[11] R. BRAUN, B. D. CASSON, C. D. BAIN, E. W. M. VAN DER HAM, Q. H. F. VREHEN, E. R. ELIEL, A. M. BRIGGS, and P. B. DAVIES, J. Chem. Phys. **110**, 4634 (1999).
[12] R. SCHLÖGL and A. ZECCHINA, in: Topics in Catalysis **15**, Special Issue on in-situ Characterization of Catalysts (2001).
[13] J. M. THOMAS and G. A. SOMORJAI, in: Topics in Catalysis **8**, Special Issue on in-situ Characterization of Catalysts (1999).
[14] X. SU, P. S. CREMER, Y. R. SHEN, and G. A. SOMORJAI, J. Am. Chem. Soc. **119**, 3994 (1997).
[15] H. HÄRLE, A. LEHNERT, U. METKA, H. R. VOLPP, L. WILLMS, and J. WOLFRUM, Chem. Phys. Lett. **293**, 26 (1998).
[16] T. DELLWIG, G. RUPPRECHTER, H. UNTERHALT, and H.-J. FREUND, Phys. Rev. Lett. **85**, 776 (2000).
[17] J. A. JENSEN, K. B. RIDER, M. SALMERON, and G. A. SOMORJAI, Phys. Rev. Lett. **80**, 1228 (1998).

[18] S. Lin, A. Oldfield, and D. Klenerman, Surf. Sci. **464**, 1 (2000).
[19] G. Rupprechter and H.-J. Freund, Topics in Catalysis **14**, 3 (2001).
[20] A. Eppler, G. Rupprechter, E. A. Anderson, and G. A. Somorjai, J. Phys. Chem. B **104**, 7286 (2000).
[21] G. Rupprechter, T. Dellwig, H. Unterhalt, and H.-J. Freund, Topics in Catalysis **15**, 19 (2001).
[22] H. Unterhalt, G. Rupprechter, and H.-J. Freund, J. Phys. Chem. B **106** (2002), in press.
[23] G. Rupprechter, T. Dellwig, H. Unterhalt, and H.-J. Freund, J. Phys. Chem. B **105**, 3797 (2001).
[24] M. Bäumer and H.-J. Freund, Prog. Surf. Sci. **61**, 127 (1999).
[25] M. Tüshaus, W. Berndt, H. Conrad, A. M. Bradshaw, and B. Persson, Appl. Phys. A **51**, 91 (1990).
[26] F. M. Hoffmann, Surf. Sci. Rep. **3**, 103 (1983).
[27] H. Conrad, G. Ertl, and J. Küppers, Surf. Sci. **76**, 323 (1978).
[28] W. K. Kuhn, J. Szanyi, and D. W. Goodman, Surf. Sci. Lett. **274**, L611 (1992).
[29] B. Bourguignon, S. Carrez, B. Dragnea, and H. Dubost, Surf. Sci. **418**, 171 (1998).
[30] S. Surnev, M. Sock, M. G. Ramsey, F. P. Netzer, M. Wiklund, M. Borg, and J. N. Andersen, Surf. Sci. **470**, 171 (2000).
[31] T. Giessel, O. Schaff, C. J. Hirschmugl, V. Fernandez, K. M. Schindler, A. Theobald, S. Bao, R. Lindsay, W. Berndt, A. M. Bradshaw, C. Baddeley, A. F. Lee, R. M. Lambert, and D. P. Woodruff, Surf. Sci. **406**, 90 (1998).
[32] A. Bandara, S. Dobashi, J. Kubota, K. Onda, A. Wada, K. Domen, C. Hirose, and S. Kano, Surf. Sci. **387**, 312 (1997).
[33] C. Klünker, M. Balden, S. Lehwald, and W. Daum, Surf. Sci. **360**, 104 (1996).
[34] H. Härle, U. Metka, H.-R. Volpp, and J. Wolfrum, Phys. Chem. Chem. Phys. **1**, 5059 (1999).
[35] S. Baldelli, N. Markovic, P. Ross, Y. R. Shen, and G. A. Somarjai, J. Phys. Chem. B **103**, 8920 (1999).
[36] K. H. Hansen, T. Worren, S. Stempel, E. Lægsgaard, M. Bäumer, H.-J. Freund, F. Besenbacher, and I. Stensgaard, Phys. Rev. Lett. **83**, 4120 (1999).
[37] K. Wolter, O. Seiferth, H. Kuhlenbeck, M. Bäumer, and H.-J. Freund, Surf. Sci. **399**, 190 (1998).
[38] M. Frank and M. Bäumer, Phys. Chem. Chem. Phys. **2**, 3723 (2000).
[39] R. K. Brandt, M. R. Hughes, L. P. Bourget, K. Truszkowska, and R. G. Greenler, Surf. Sci. **286**, 15 (1993).
[40] D. R. Rainer, M.-C. Wu, D. I. Mahon, and D. W. Goodman, J. Vac. Sci. Technol. A **14**, 1184 (1996).
[41] P. Gelin, A. Siedle, and J. Yates, J. Phys. Chem. **88**, 2978 (1984).